JOURNAL OF APPLIED PHYSICS VOLUME 95, NUMBER 10 15 MAY 2004

Strain relaxation and threading dislocation density in helium-implanted and annealed $Si_{1-x}Ge_x$/Si(100) heterostructures

J. Cai, P. M. Mooney, and S. H. Christiansen[a)]
IBM Research and Development Center, T. J. Watson Research Center, Yorktown Heights, New York 10598

H. Chen
IBM Research and Development Center, Microelectronics Division, Hopewell Junction, New York 12533

J. O. Chu and J. A. Ott
IBM Research and Development Center, T. J. Watson Research Center, Yorktown Heights, New York 10598

(Received 22 January 2004; accepted 16 February 2004)

Strain relaxation and threading dislocation densities in $Si_{1-x}Ge_x$ ($0.15<x<0.30$) produced by He implantation and annealing have been investigated using x-ray diffraction and transmission electron microscopy. The degree of strain relaxation is very sensitive to the SiGe layer thickness; only small differences in strain relaxation are obtained when the helium dose and energy are varied over a relatively wide range. In contrast, the threading dislocation density is strongly influenced by the implantation dose and depth. A composite parameter, the He dose in the SiGe layer (He(SiGe)), calculated from He profiles simulated using the program Stopping and Range of Ions in Matter (SRIM2000), correlates well with the threading dislocation density. We have found that to achieve a low threading dislocation density, $<5\times10^7$ cm^{-2}, He(SiGe) must be less than 1×10^{15} cm^{-2}.
 [DOI: 10.1063/1.1699488]

I. INTRODUCTION

Strain-relaxed $Si_{1-x}Ge_x$ alloys are used as virtual substrates for strained Si devices in which the electron and hole mobility is enhanced compared to devices fabricated in unstrained Si.[1,2] When SiGe layers are grown epitaxially on Si(001) substrates, the strain is relaxed by plastic deformation, i.e., misfit dislocations are formed when the strain in the layers exceeds the critical value.[3–5] Ideally, misfit dislocations would be nucleated and would glide to the edge of the sample, leaving a network of misfit dislocations at interfaces. However, in practice a large number of dislocations are nucleated. After gliding a short distance they become immobilized, resulting in SiGe layers with a very high density of threading dislocations.

In order to achieve useful materials for device applications, we need to find methods to produce SiGe layers with the following properties: a high degree of strain relaxation, a low threading dislocation density, and a flat surface. Traditionally, device-quality relaxed SiGe buffer layers have been achieved by growth of a very thick compositionally graded $Si_{1-x}Ge_x$ layer on Si. Nearly completely relaxed $Si_{1-x}Ge_x$ ($0.1<x<1$) with threading dislocation densities of 1×10^5–5×10^7 cm^{-2} have been demonstrated.[6,7] Despite the low threading dislocation density, there are problems when using these layers for CMOS applications. First, these layers have rough surfaces, typically a root mean square (RMS) surface roughness of ~6 nm when $x=0.3$. Therefore an extra process to planarize the surface, for example, chemical–mechanical polishing, has to be applied before growing device structures, thus increasing the cost. In addition, the thermal conductivity of SiGe is lower than that of pure Si. Therefore using a thick graded buffer layers result in poor heat conductivity, which may be troublesome for applications in ultra-large-scale integrated circuits.

It is well known that ion-implantation into SiGe enhances strain relaxation. For example, regions of SiGe layers implanted with B or As relax more upon annealing than do regions that were not implanted.[8] In another example, misfit dislocations were found to nucleate preferentially during growth of SiGe layers in regions where the Si substrate had been implanted with Ge.[9] More recently, ion implantation of He and H_2 were proposed as an alternative way to obtain high quality SiGe buffer layers. The core idea is to implant H_2 or He into pseudomorphic SiGe layers to introduce a damage layer below the SiGe/Si interface.[10,11] During subsequent annealing, dislocations nucleated in the damage layer glide or climb to the SiGe/Si interface and relieve the mismatch strain. It was reported that thin SiGe layers having a high degree of relaxation as well as relatively low threading dislocation density can be achieved by helium implantation and subsequent annealing at temperatures of 750 °C–850 °C.[10–12]

We have studied strain relaxation and the defect density of SiGe buffer layers produced by He implantation and annealing. An initial transmission electron microscopy (TEM) study of 100 nm thick $Si_{1-x}Ge_x$ ($x=0.15$) layers, showed that the implant damage, and also the relaxation mechanism, varies with implantation conditions, even though the degree of strain relaxation was found to be similar.[12] Here we present results of a larger study of the effects of experimental parameters such as SiGe layer thickness and alloy composition and implantation conditions on the properties of SiGe virtual substrates. We find that the degree of strain relaxation

[a)]Present address: MPI-Mikrostrukturphysik, Halle, Germany.

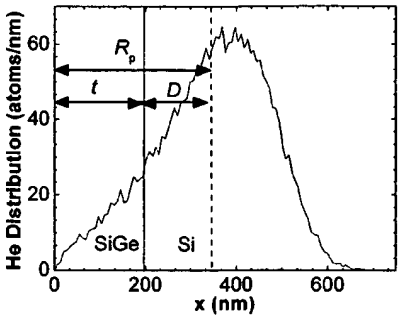

FIG. 1. A simulated helium profile of 38 keV He^+ implanted into a 196 nm $Si_{0.7}Ge_{0.3}$/Si structure. R_p is the projected range of He, and t is the SiGe layer thickness, and D is the implantation depth with respect to the SiGe/Si interface. The total number of He atoms used in the simulation is 20 000.

is strongly dependent on the SiGe layer thickness and only weakly dependent on the He dose and depth. In contrast, we also find that the threading dislocation density is very sensitive to the He implantations conditions. There is a strong correlation between the amount of He implanted into the SiGe layer, He(SiGe), and the threading dislocation density.

II. EXPERIMENTAL METHODS

Pseudomorphic $Si_{1-x}Ge_x$ layers ($0.15<x<0.30$) were grown on Si (100) by ultrahigh vacuum chemical vapor deposition (UHVCVD) on 200 mm Si(001) substrates and by rapid thermal chemical vapor deposition (RTCVD) on both 200 and 300 mm Si(001) substrates. He^+ ions were then implanted into the wafers at room temperature. The implantation energy was chosen so that the projected range (R_p) of He atoms obtained using the simulation software SRIM2000 is below the SiGe/Si interface. Figure 1 shows a simulated helium profile for a 196 nm thick $Si_{0.7}Ge_{0.3}$ layer on a Si substrate implanted with 38 keV He^+. In order to compare SiGe layers of different thickness, we define a parameter D, the implantation depth below the SiGe/Si interface, as R_p minus t, the SiGe layer thickness. After implantation, wafers were annealed in a He or N_2 ambient, at a temperature of 800 °C or 850 °C for 12 minutes or longer.

High-resolution x-ray diffraction (XRD) was used to measure layer thickness and Ge composition of the as-grown pseudomorphic SiGe layers at the wafer center, and also the degree of strain relaxation of the SiGe layer in each sample after annealing. X-ray measurements were performed using a Philips XPert Pro diffraction system equipped with a hybrid incident beam monochromator consisting of a mirror and a four-bounce Ge crystal that gives a 1 mm×10 mm incident Cu–K_α beam ($\lambda=1.542$ Å) with a divergence of 0.007°. For the relaxed layers, both symmetric (004) and asymmetric (224) reflections were measured by XRD. The degree of strain relaxation was calculated by

$$\%\ \text{strain relaxation}=\frac{a_l-a_s}{a_l^R-a_s}\times 100\%,$$

where a_l and a_s are the in-plane lattice constants of the $Si_{1-x}Ge_x$ layer and the Si substrate, respectively, and a_l^R is the lattice constant of fully relaxed $Si_{1-x}Ge_x$. The uncertainty in the Ge mole fraction is ±0.01 and in the strain relaxation is ±3%. Surface features were measured by atomic force microscopy (AFM) using a Digital Instruments Dimension 5000 Nanoscope. Plan-view transmission electron microscopy (PVTEM) was used to determine the threading dislocation density. TEM samples were prepared by standard mechanical thinning and ion milling techniques. The observations were performed in a CM12 microscope operating at 120 kV. Threading dislocations were counted in an area of 360 μm^2 for samples with a density of 10^7 cm^{-2}, with a typical uncertainty of ±30%.

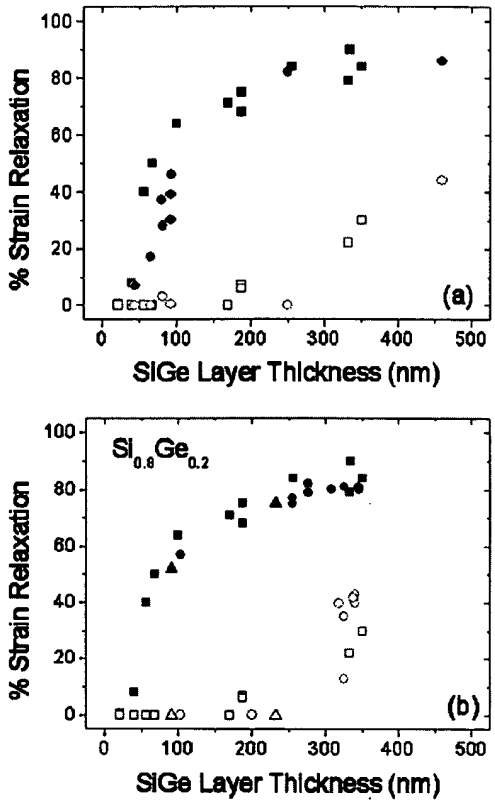

FIG. 2. (a) Strain relaxation of $Si_{1-x}Ge_x$ layers, $x=0.16$ (●○) and $x=0.20$ (■□), grown by UHVCVD on 200 mm wafers. (b) Strain relaxation of $Si_{0.8}Ge_{0.2}$ layers grown in three different reactors: UHVCVD-200 (■□); RTCVD-200 (●○); and RTCVD-300 (▲△). Samples were annealed at 800 °C or 850 °C for at least 10 minutes. Open symbols are areas of the wafer that were not implanted. Solid symbols are areas that were implanted with 1×10^{16} cm^{-2} helium at a depth of 140–200 nm below the SiGe/Si interface. The error in the strain relaxation measured by XRD is ~±3%.

III. RESULTS AND DISCUSSION

The relationship between strain relaxation and SiGe layer thickness is shown in Fig. 2. Figure 2(a) compares $Si_{1-x}Ge_x$ samples with $x=0.15$ and $x=0.20$ grown by UHVCVD. The He^+ dose was the same, 1×10^{16} cm^{-2}, for all these samples and the implantation energy was varied to give a depth, D, of 140–200 nm. For both alloy compositions, the degree of strain relaxation increases with the layer thickness, saturating at a value of ~85%. A high degree of strain relaxation (>70%) is achieved only when the SiGe thickness is >200 nm. The scatter in the data is due to the variation of

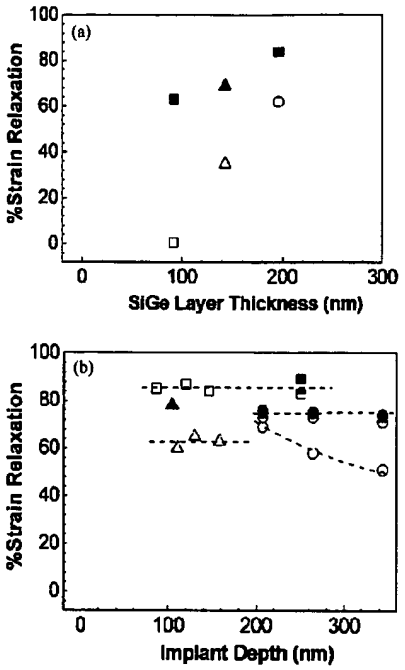

FIG. 3. (a) Strain relaxation of $Si_{1-x}Ge_x$ layers grown by RTCVD, $x = 0.3$. Open symbols are areas of the wafer that were not implanted. Solid symbols are areas that were implanted with 10^{16} cm^{-2} helium at a depth of 150–200 nm below the SiGe/Si interface. (b) Relaxation of $Si_{0.7}Ge_{0.3}$ layers with different thickness and implantation conditions. ■□, ●○, and ▲△ represent 196, 143, and 92 nm SiGe layers, respectively. Open, half-filled and filled symbols represent helium implantation doses of 1, 1.5, and 2 $\times 10^{16}$ cm^{-2}, respectively.

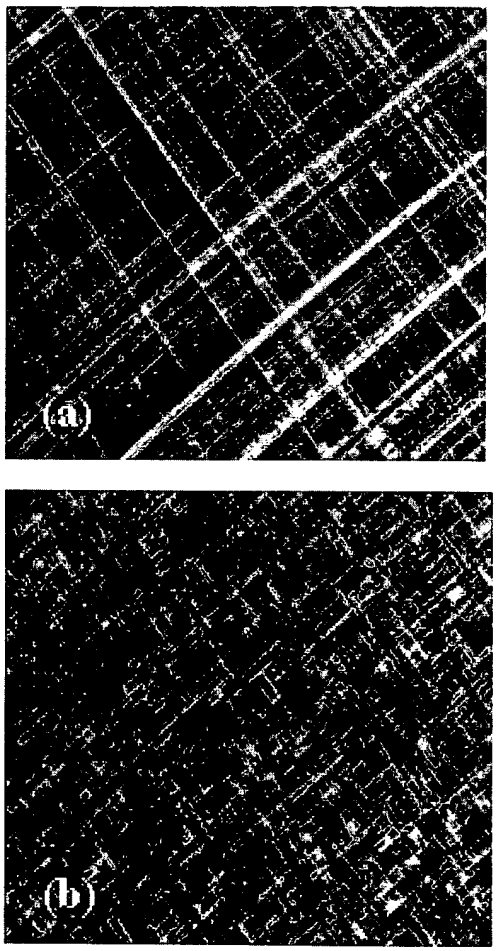

FIG. 4. AFM images of two types of surface features in implanted/annealed 196 nm $Si_{0.7}Ge_{0.3}$ layers: (a) regular cross-hatch patterns for deeper implanted samples ($D = 146$ nm) and (b) patchy patterns for shallower implanted samples ($D = 86$ nm). Helium dose is 10^{16} cm^{-2} in both cases. The images shown have an area of 15×15 μm^2.

the SiGe layer thickness across the wafer. The degree of strain relaxation was found to be the same for annealing at both 800 °C and 850 °C and for times of 12–60 minutes. Comparing with pieces of the wafer that were not implanted but were annealed under the same conditions, He implantation before annealing greatly enhances the strain relaxation, even for the thickest SiGe layers. Figure 2(b) compares $Si_{0.8}Ge_{0.2}$ samples grown by UHVCVD and RTCVD. Again the He^+ dose and implant depth, D, were similar for all the samples. Clearly the degree of strain relaxation is the same for samples grown by both methods.

Figure 3(a) compares $Si_{0.7}Ge_{0.3}$ layers with and without He implants after annealing. The He dose was 1×10^{16} cm^{-2} and the depth, D, was 150–200 nm. Again we see that the degree of strain relaxation increases with the layer thickness and is enhanced by the He implant. Figure 3(b) shows the effects of varying the He implantation dose and depth on the strain relaxation of $Si_{0.7}Ge_{0.3}$. The strain relaxation of thick films ($t = 196$ nm) is about 85%, and it is insensitive to the implantation depth and dose. For thinner films, increasing the He dose affects the degree of strain relaxation. This is shown for 143 nm thick films with very deep implants and for 92 nm thick films with very shallow implants. However, the total degree of relaxation of ion-implanted samples is much more sensitive to the SiGe layer thickness than to the He^+ implantation conditions.

The surfaces of ion implanted and annealed buffer (IAB) layers are relatively smooth. The root mean square surface roughness is in the range of 0.2–0.6 nm. However, we have also observed two types of surfaces on the IAB layers. Both types of surfaces show straight-line cross-hatch features running along perpendicular [110] axes, which correspond to the misfit dislocations that relieve the strain.[13] One type of surface, shown in Fig. 4(a), exhibits a pattern of long, straight lines indicating the presence of long misfit dislocations, whereas the other type, shown in Fig. 4(b), exhibits a patchy surface of short straight lines indicating the presence of much shorter misfit dislocations in these samples. Although the RMS roughness of these two types of surfaces is quite similar and the degree of strain relaxation in both types of samples is comparable, the threading dislocation densities in these SiGe layers are very different. Consistent with the observation of short misfit dislocations, PVTEM images show that samples with patchy surfaces always have a very high density of threading dislocations ($>10^9$ cm^{-2}).

Figure 5 compares misfit dislocations in two $Si_{0.7}Ge_{0.3}$ samples with similar strain relaxation (~75%) but very different surface features. The sample with deep helium implantation has an array of long, straight misfit dislocations at the

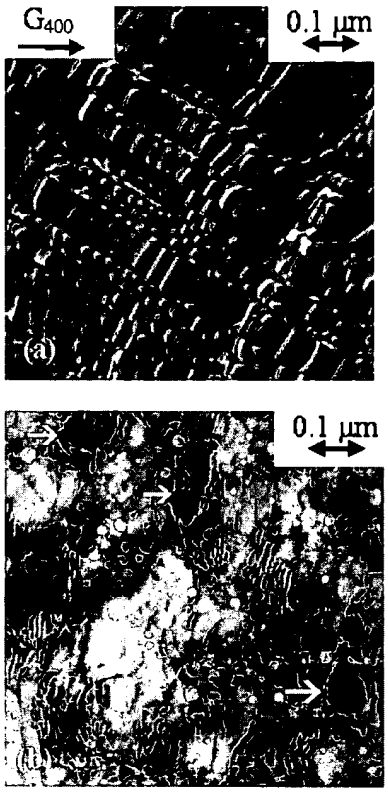

FIG. 5. Plan-view TEM images of samples with low and high threading dislocations. (a) Dark field image shows the regular array of misfit dislocations in a 143 nm $Si_{0.7}Ge_{0.3}$ layer with threading dislocation density of 4.4×10^7 cm^{-2}. The material is 74% relaxed after annealing. (b) Bright field image taken at weak diffraction conditions shows both helium bubbles and the irregular misfit dislocation array in a 92 nm $Si_{0.7}Ge_{0.3}$ layer with threading dislocation density of 2.7×10^{10} cm^{-2}. The material is 78% relaxed after annealing. Dark contrast areas indicated by arrows are regions of very high strain.

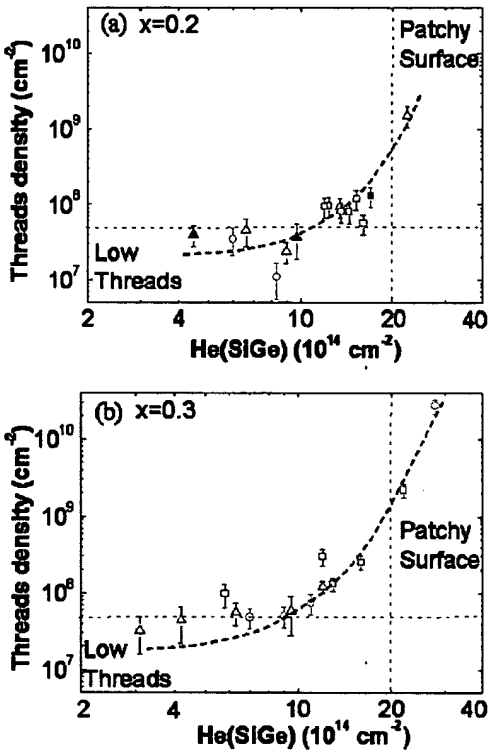

FIG. 6. Threading dislocation density increases with He(SiGe). Open and solid symbols are wafers grown by RTCVD and UHVCVD, respectively. Dashed lines are guides for the eye. (a) Threading dislocation density in $Si_{0.8}Ge_{0.2}$ layers, O are 92 nm, 52% relaxed; ▲△ are 220 nm, 70% relaxed; ■□ are 320–340 nm, 80% relaxed. (b) Threading dislocation density in $Si_{0.7}Ge_{0.3}$ layers, O are 92 nm, 60% relaxed; △ are 143 nm, 70% relaxed; □ are 196 nm, 85% relaxed.

SiGe/Si interface, shown in Fig. 5(a), and it has a surface similar to Fig. 4(a). This SiGe layer has a relatively low threading dislocation, 4.4×10^7 cm^{-2}. In contrast, Fig. 5(b) shows a high density of helium bubbles and an irregular array of misfit dislocations in a sample with shallow helium implantation. This sample has a very high density of threading dislocations, 2.7×10^{10} cm^{-2}, and its surface looks like that in Fig. 4(b).

Comparing samples with a variety of implant doses and implant depths, we have found that the amount of He implanted into the SiGe layer correlates strongly with the threading dislocation density. We introduce a parameter, the amount of He in the SiGe layer, as a measure of the damage in the SiGe layer caused by the He implantation. He(SiGe) is defined as the integral of the He profile over the SiGe layer thickness, i.e., $\int_0^t [\mathrm{He}]dx$. For example, the He dose in the SiGe layer shown in Fig. 1 is 12% of the total implanted He dose.

Figure 6 shows the threading dislocation density plotted against He(SiGe) for both UHVCVD and RTCVD grown $Si_{1-x}Ge_x$ layers. The threading dislocation density increases strongly with He(SiGe). When the amount of He increases by one order of magnitude, from 3×10^{14} cm^{-2} to 4×10^{15} cm^{-2}, the threading dislocation density increases by three orders of magnitude. Figure 6(a) shows the plot for $Si_{0.8}Ge_{0.2}$ layers; whenever He(SiGe) is greater than 2×10^{15} cm^{-2}, the threading dislocation density is higher than 10^9 cm^{-2}, and samples have patchy surfaces like that shown in Fig. 4(b). In contrast, a low threading dislocation density ($< 5 \times 10^7$ cm^{-2}) is obtained when He(SiGe) is $< 10^{15}$ cm^{-2}. A similar behavior is seen for $Si_{0.7}Ge_{0.3}$ layers in Fig. 6(b). *Both plots suggest that the lower limit for the threading dislocation density is* $\sim 10^7$ cm^{-2}.

Figure 6 also shows that layers with a high degree of strain relaxation are not always companied by high density of threading dislocations. Take for instance Fig. 6(b): The 143 nm $Si_{0.7}Ge_{0.3}$ layers have a higher degree of relaxation than the 92 nm layers, but the threading dislocation density in the 143 nm layers is lower. Therefore, by carefully choosing layer thickness and implantation conditions, SiGe layers with both a high degree of strain relaxation and a relatively low density of threading dislocation can be produced by He implantation and annealing.

We now turn to a brief discussion of strain relaxation mechanisms. It is known from earlier work that He implanted below the SiGe/Si interface agglomerates into bubbles and/or platelets during annealing, and dislocation loops are punched out around them.[11] These loops glide or climb to the SiGe/Si interface, and misfit dislocations that

relieve the mismatch strain in the SiGe layer are formed.[11,12] Because helium implantation and annealing provides a high density of nucleation sources for dislocations, the strain relaxation in the SiGe layer is enhanced compared to samples with no implant. Provided there are enough dislocation sources, the final degree of strain relaxation depends on the initial elastic strain energy in the film, which in turn only depends on the layer thickness, for layers with a given germanium composition.[14–18] This explains our observation that the degree of relaxation in the thicker SiGe layers depends only on the layer thickness, even though the He implantation conditions are different. However, in the case of thinner layers where there is a lower driving force for strain relaxation, increasing the He dose or reducing the implantation depth slightly increases the degree of strain relaxation, as shown in Fig. 3(b). For a given SiGe layer thickness, reducing the implant depth and/or increasing the implant dose increases the value of He(SiGe), and also results in a high threading dislocation density. When He(SiGe) is relatively high, two mechanisms may cause a high threading dislocation density in SiGe. One possibility is that a large number of dislocation loops are nucleated at SiGe.Si interfaces layer during annealing because of the high concentration of helium bubbles there. Since the density of loops is very high, each one will be able to glide for only a short distance, before reaching an area of low strain. Alternatively, the high density of bubbles or other implantation damage at the interfaces may impede dislocation glide, forcing additional misfit dislocation nucleation to occur in order to relieve the strain. In either case, the end result will be short misfit dislocations and a very high density of threading dislocations. In contrast, higher-dose deeper implants are better solutions, because they provide increased strain relaxation as well as a relatively low density of threading dislocations. Our observation of a lower limit of 1×10^{7} cm^{-3} for the threading dislocation density suggests that dislocation interactions play an important role in strain relaxation, as has also been shown by numerical simulations.[19]

IV. CONCLUSIONS

We have demonstrated in this study that highly relaxed $Si_{1-x}Ge_x$ layers (>75%) with a RMS surface roughness <0.6 nm, and threading dislocation density less than 5 $\times10^{7}$ cm^{-2} can be achieved by helium implantation and annealing. The degree of strain relaxation and the defect density in the final SiGe layers are similar for layers grown by UHVCVD and RTCVD. We find that the layer thickness and the amount of helium implanted into SiGe are two key parameters, which greatly influence the degree of strain relaxation and the threading dislocation density, respectively. Our results also suggest that 10^{7} cm^{-2} is the lower limit for the threading dislocation density in He implanted and annealed SiGe buffer layers.

ACKNOWLEDGMENTS

We gratefully acknowledge the assistance of D.L. Lacey with XRD measurements, and P.A. Saunders with helium implantations.

[1] K. Ismail, B. S. Meyerson, and P. J. Wang, Appl. Phys. Lett. **58**, 2117 (1991).
[2] Y. J. Mii, Y. H. Xie, E. A. Fitzgerald, D. Monrow, F. A. Thiel, B. E. Weir, and L. C. Feldman, Appl. Phys. Lett. **59**, 1611 (1991).
[3] J. H. Van der Merwe, J. Appl. Phys. **34**, 117 (1963).
[4] J. H. Van der Merwe, J. Appl. Phys. **34**, 123 (1963).
[5] E. A. Fitzgerald, Mater. Sci. Rep. **7**, 87 (1991).
[6] F. K. LeGoues, B. S. Meyerson, J. F. Morar, and P. D. Kirchner, J. Appl. Phys. **71**, 4203 (1992).
[7] E. A. Fitzgerald, Y.-H. Xie, D. Monroe, P. J. Silverman, J. M. Kuo, A. R. Kortan, F. A. Thiel, and B. E. Weir, J. Vac. Sci. Technol. B **10**, 1807 (1992).
[8] R. Hull, J. C. Bean, J. M. Bonar, G. S. Higashi, K. T. Short, H. Temkin, and A. E. White, Appl. Phys. Lett. **56**, 2445 (1990).
[9] J. P. Watson, E. A. Fitzgerald, Y.-H. Xie, P. J. Silverman, A. E. White, and K. T. Short, Appl. Phys. Lett. **63**, 764 (1993).
[10] S. Mantl, B. Holländer, R. Liedtke, St. Mesters, H.-J. Herzog, H. Kibbel, and T. Hackbarth, Nucl. Instrum. Methods Phys. Res. B **147**, 29 (1999).
[11] M. Luysberg, D. Kirch, H. Trinkaus, B. Holländer, St. Lenk, S. Mantl, H.-J. Herzog, T. Hackbarth, and P. F. P. Fichtner, J. Appl. Phys. **92**, 4290 (2002).
[12] S. H. Christiansen, P. M. Mooney, J. O. Chu, and A. Grill, Mater. Res. Soc. Symp. Proc. **686**, 27 (2002).
[13] M. A. Lutz, R. M. Feenstra, F. K. LeGoues, P. M. Mooney, and J. O. Chu, Appl. Phys. Lett. **66**, 724 (1995).
[14] J. H. van der Merwe, Surf. Sci. **31**, 198 (1972).
[15] J. H. van der Merwe and C. A. B. Ball, in *Epitaxial Growth*, edited by J. W. Matthews (Academic, New York, 1975), Part B, Chap. 6.
[16] J. W. Mathews, J. Vac. Sci. Technol. **12**, 126 (1975).
[17] J. W. Mathews, in *Epitaxial Growth*, edited by J. W. Mathews (Academic, New York, 1975), Part B, Chap. 8.
[18] J. W. Mathews, in *Dislocations in Solids*, edited by F. R. N. Nabarro (North-Holland, Amsterdam, 1979).
[19] K. W. Schwarz, Phys. Rev. Lett. **91**, 145503 (2003).

Effect of helium ion implantation and annealing on the relaxation behavior of pseudomorphic $Si_{1-x}Ge_x$ buffer layers on Si (100) substrates

M. Luysberg,[a] D. Kirch, and H. Trinkaus
Institut für Festkörperforschung, Forschungszentrum Jülich GmbH, D-52425 Jülich, Germany

B. Holländer, St. Lenk, and S. Mantl
Institut für Schichten and Grenzflächen, Forschungszentrum Jülich GmbH, D-52425 Jülich, Germany

H.-J. Herzog and T. Hackbarth
Daimler-Chrysler AG, Research and Technology, D-89081 Ulm, Germany

P. F. P. Fichtner
Departamento de Metalurgia, Universidad Federal do Rio Grande do Sul, P.O. Box 15051, 91501-970 Porto Alegre, RS, Brazil

(Received 19 April 2002; accepted for publication 10 July 2002)

The influence of He implantation and annealing on the relaxation of $Si_{0.7}Ge_{0.3}$ layers on Si (100) substrates is investigated. Proper choice of the implantation energy results in a narrow defect band $\approx$100 nm underneath the substrate/epilayer interface. During annealing at 700–1000 °C, He-filled bubbles are created, which act as sources for misfit dislocations. Efficient annihilation of the threading dislocations is theoretically predicted, if a certain He bubble density with respect to the buffer layer thickness is maintained. The variation of the implantation dose and the annealing conditions changes density and size of spherical He bubbles, resulting in characteristic differences of the dislocation structure. $Si_{1-x}Ge_x$ layers with Ge fractions up to 30 at. % relax the initial strain by 70% at an implantation dose of 2×10^{16} cm^{-2} and an annealing temperature as low as 850 °C. Simultaneously, a low threading dislocation density of 10^7 cm^{-2} is achieved. The strain relaxation mechanism in the presence of He filled bubbles is discussed. © *2002 American Institute of Physics.* [DOI: 10.1063/1.1504496]

I. INTRODUCTION

"Virtual" substrates in the form of strain relaxed and rather defect-free $Si_{1-x}Ge_x$ layers on Si (100) are the key to control the strain and, by that, the band gap and band offset of Si/SiGe layers grown onto such substrates. Following this concept, highly attractive heterostructures such as hetero-field-effect transistors (FETs) can be fabricated.[1–3] The promising application in high speed electronic devices based on Si technology has triggered many efforts to tackle the basic problem: Initially, $Si_{1-x}Ge_x$ layers deposited onto Si (100) substrates below the critical thickness are metastable, dislocation free, and tetragonally strained according to the lattice mismatch. On the one hand, these $Si_{1-x}Ge_x$ layers have to be transformed into the relaxed state without introducing a significant density of threading dislocations piercing the active device area. On the other hand, for many applications the Ge content has to be increased up to a value of 50% to provide optimum band gap and band offset values. Conventional relaxation methods like thermal annealing result in only a low degree of relaxation accompanied by a high density of detrimental threading dislocations, and are therefore not the method of choice.[4,5]

Many approaches have been developed to reduce the density of surface penetrating threading dislocations: By growth of several μm thick compositionally graded SiGe alloy layers[6,7] the threading dislocation density in SiGe (30%) buffers was reported to be as low as 10^4–10^7 cm^{-2}. Alternatively, thick $Si_{1-x}Ge_x$ layers were grown on very thin Si surface films of silicon-on-insulator wafers, which causes the threading dislocations to bend down toward the Si/SiO_2 interface, thus preventing a high threading dislocation density in the $Si_{1-x}Ge_x$ layer.[8] Thin strain relaxed SiGe buffer layers were formed by ion implantation of Ge into the thin Si layers of silicon-on-insulator substrates, where thermal annealing led to homogeneous $Si_{1-x}Ge_x$ layers directly on SiO_2.[9] In other approaches, SiGe buffer layers were deposited onto a low-temperature grown Si or SiGe buffer layer,[10,11] where the high intrinsic defect density injected into the low temperature layer enhances the nucleation of strain-relieving misfit dislocations and reduces the threading dislocation density considerably. However, successful results were only obtained for rather low Ge concentrations (<20%). A comparison of device properties of modulation doped quantum wells and FETs grown onto different types of SiGe buffers shows thick graded buffers to be better than low-temperature buffers, both of them being superior to constant composition buffers.[12]

Recently, high degrees of relaxation and low threading dislocation densities were achieved by H and He implantation and subsequent annealing of thin $Si_{1-x}Ge_x$ layers on Si (100) substrates.[13–15] The main advantage of this technique is that thin, strain-relaxed SiGe layers, which are produced by use of overpressurized H or He bubbles acting as internal dislocation sources, can be processed by simple, standard

[a]Author to whom correspondence should be addressed; electronic mail: m.luysberg@fz-juelich.de

TABLE I. Summary of He implantation doses, annealing temperatures and times, and quantitative results of the structural analyses. All samples consist of a 100 nm thick $Si_{0.7}Ge_{0.3}$ layer grown onto Si (100) substrate.

Implantation dose (10^{16} cm^{-2})	Annealing temperature/time (°C)/(s)	Degree of relaxation (%)	Diameter of He bubbles (nm)	Mean distance of He bubbles (nm)	Threading dislocation density (10^7 cm^{-2})
0	750/600	7	...	...	...
	800/600	14	...	...	...
	850/600	34	...	...	...
	1000/30	34	...	...	...
1.2	850/600	70	15.1±4.9	49.5	45±1.8
2.0	as implanted	...	no bubbles observed	...	no dislocations observed
	750/600	66	8.59±4.59	9.3	3.7±1.8
	800/600	68	10.78±4.06	12.6	4.4±1.6
	850/600	68	15.39±4.89	18.3	1.62±0.8
	1000/30		22.99±6.96	24.1	102±39
2.8	850/600	83	15.92±5.61	13.8	181±1
3.0	850/600	80	13.4±3.63	13.7	7900±140
	1000/30			38.5	

technology steps. Depending on the implantation conditions, various types of He bubbles connected with different dislocation reactions were observed.[16] The interaction between bubbles and dislocations require the bubble layer to be separated from the interfacial region, i.e., best results are achieved if the bubbles are located below the interface.[15] Whereas H implantation has been found to be suitable for Ge concentration of up to about 20% only,[13] He implantation led to a successful relaxation of $Si_{1-x}Ge_x$ layers with higher Ge concentration of 30%.

In our article we investigate the relaxation behavior of $Si_{1-x}Ge_x$ layers on Si (100) substrates in dependence on He implantation and annealing conditions. The relaxation mechanism and He bubble formation are discussed on the basis of experimental results of structural characterizations by transmission electron microscopy (TEM).

II. EXPERIMENT

Metastable $Si_{1-x}Ge_x$ layers with Ge fractions of 30 at. % and a thickness of 100 nm, slightly below the critical thickness for pseudomorphic layer growth, were grown by molecular beam epitaxy on Si (100) standard wafers. The layers were fully strained according to the mismatch of −1.2% as determined by x-ray diffraction and ion channeling.[14] The heterostructures were implanted with He^+ ions with energies of 18 keV and doses in the range of 1.0×10^{16}–3.0×10^{16} cm^{-2} at room temperature with an implantation rate of 8×10^{12} cm^{-2} s^{-1}. The implantation energy was chosen such that a defect region at the end-of-range formed about 100 nm below the SiGe/Si interface.

After ion implantation the samples were annealed at 750–850 °C for 600 s or—in high-temperature samples—at 1000 °C for 30 s in a quartz lamp furnace under Ar atmosphere. For comparison, identical samples were annealed without ion implantation. The implantation and annealing conditions are summarized in Table I. The amount of strain relaxation was determined by ion channeling angular scans along a (100) plane through an inclined [110] direction and by x-ray diffraction.[14] The structural properties were investigated by use of a JEOL 4000FX TEM operated at 400 kV. Samples were prepared in cross section and in plan view by conventional techniques including Ar ion milling.

III. RESULTS

The effect of He implantation and subsequent annealing at 850 °C on the formation of He bubbles[17] in SiGe/Si heterostructures is shown in the TEM bright field images in Fig. 1. All images are taken with kinematical imaging conditions in underfocus, which causes a bright contrast of the bubbles surrounded by dark Fresnel contours. Strain fields, e.g., of dislocations appear as blurred dark contrast under these imaging conditions. The cross section viewgraph in Fig. 1(a) reveals a well defined layer of spherical bubbles in a sample

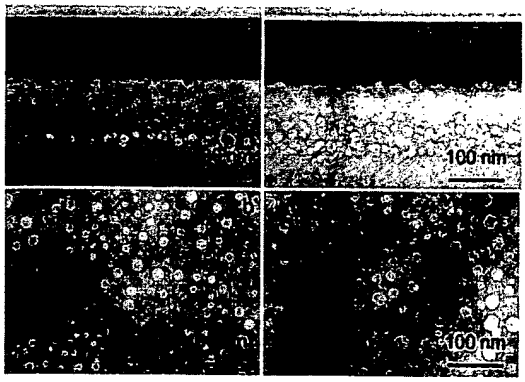

FIG. 1. The bright field electron micrographs show the $Si_{0.7}Ge_{0.3}$/Si(100) heterostructures in cross section and plan-view. Upon He implantation with 2×10^{16} cm^{-2} and annealing at 850 °C (a) and (b) a well defined bubble layer of laterally homogeneously distributed bubbles is observed. Implantation with 2.8×10^{16} cm^{-2} and annealing at 850 °C (c) and (d) results in a broadening of the bubble layer and the formation of bubbles within the interface.

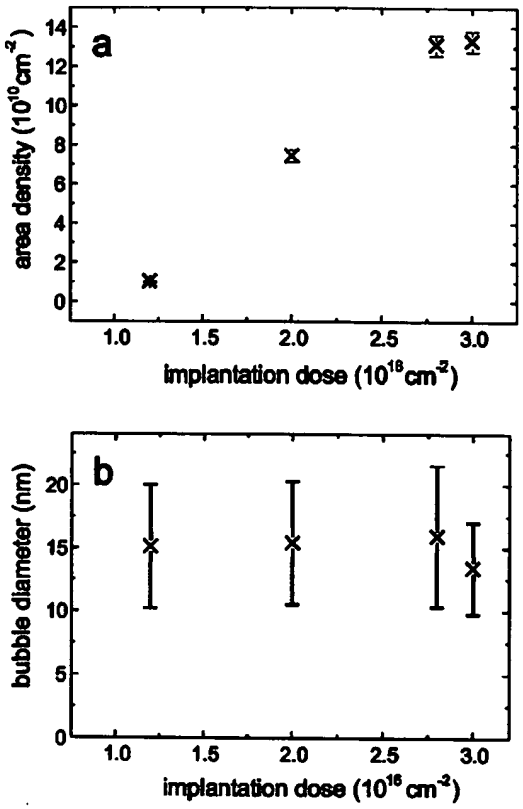

FIG. 2. The area density (a) and bubble diameter (b) are plotted vs the implantation dose. The annealing temperature of 850 °C is the same for all samples.

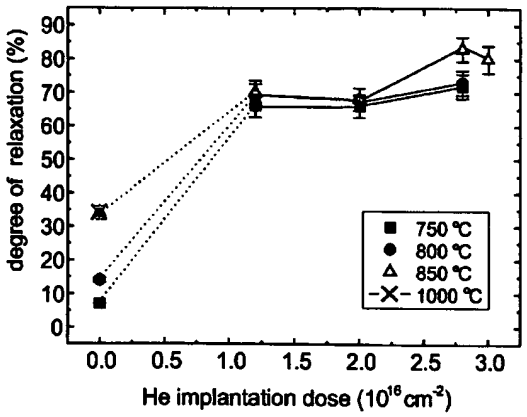

FIG. 3. Degree of relaxation vs the He implantation dose for the different annealing temperatures indicated. Samples at 0 cm^{-2} were not implanted but annealed only.

implanted with 2×10^{16} cm^{-2} He. According to the ion energy chosen, the layer is located about 100 nm below the SiGe/Si interface, i.e., within the Si substrate. A homogeneous lateral distribution of the bubbles is deduced from the corresponding plan-view image shown in Fig. 1(b). The shape of the bubbles is almost spherical with diameters ranging from 5 to 25 nm. Applying a higher implantation dose of 2.8×10^{16} cm^{-2} results in a considerably broader bubble layer as depicted in the cross sectional viewgraph [Fig. 1(c)]. Furthermore, large bubbles are located within the interface of the SiGe/Si heterostructure. Dark contrast within the SiGe epilayer is caused by threading dislocations. In plan view, again, a homogeneous distribution of the bubbles is detected. However, the density of the bubbles is considerably higher in Fig. 1(d) compared to the lower dose [Fig. 1(b)] imaged with the same magnification. The size of the spherical bubbles is about the same. Dynamical two beam imaging conditions were applied to investigate strain fields. It has to be emphasized that the bubbles do not show any strain contrast, and are therefore surrounded by an undistorted Si matrix. Few dislocations were found to be attached to some of the bubbles.

Quantitative assessment of the bubble density and size is shown in Fig. 2 for samples subjected to different implantation doses, while the annealing temperature (850 °C) and time (10 min) were the same for all cases. The area density of the bubbles determined form plan-view electron micrographs is plotted in Fig. 2(a), which allows the comparison between samples with different, partly inhomogeneous depth distributions of the bubble layer [see e.g., Figs. 1(a) and 1(b)]. Clearly, an increase of the bubble density is observed for increasing implantation dose. The mean lateral distance of the He bubbles determined form the area density is given in Table I. These values reflect the "real" distance between precipitates, if the bubble layer is thin, i.e., at implantation doses $\leq 2\times10^{16}$ cm^{-2} and annealing temperatures $\leq$850 °C. As the bubble layer becomes thicker, the distance between bubbles is underestimated. The mean bubble diameter determined from measurements on about 200 bubbles in each sample remains constant with increasing He implantation dose [Fig. 2(b)]. The size of the error bars reflects the considerable scatter of bubble diameters within individual samples.

He implantation has a dramatic effect on the degree of relaxation of the SiGe layers grown on Si substrates. Figure 3 (and Table I) shows the degree of relaxation for samples subjected to different He implantation doses and annealing conditions. The values determined by Rutherford backscattering spectrometry from the Ge backscattered signal in angular scans are identical within the margin of errors with those measured by x-ray diffraction.[14] For comparison, data obtained by annealing without prior He implantation are included in the figure. Here, the maximum degree of relaxation of 35% is obtained for annealing temperatures larger than 800 °C. Considerably higher values are observed in He implanted and annealed samples. For all implantation doses and annealing temperatures applied, the degree of relaxation remains approximately constant at about 70%, except for the samples implanted at high doses and annealed at 850 °C, where even higher values of up to 83% are observed.

These high degrees of relaxation are accompanied by a high density of misfit dislocations located within the interface between the SiGe epilayer and the Si substrate. In all cases a regular dislocation network is revealed, the plan-view image in Fig. 4 being an example, where dislocations show bright contrast according to the weak beam dark field imaging conditions chosen. In this particular sample implanted

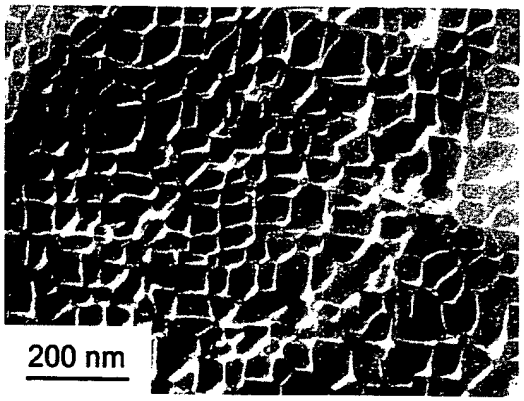

FIG. 4. Weak beam dark field electron micrograph displaying the misfit dislocation network. Dislocations show white contrast. Frequently, He bubbles can be seen to decorate the nodes of the network (arrows).

with 2×10^{16} cm^{-2} He and annealed at 1000 °C, a large number of bubbles is located within the interface, predominantly attached to the nodes of the network (see arrows in Fig. 4). Detailed contrast analyses reveal that the network consists mainly of 60° dislocations. In addition, some 90° dislocation are formed by reaction of two 60° dislocations with different Burgers vectors.

From a device point of view not only a high degree of relaxation is important but also low threading dislocation densities. The threading dislocation density was determined from plan-view samples where the Si substrate was removed. The result of counting the number of dislocations within a defined area of samples subjected to different He implantation doses and annealing temperatures is presented in Fig. 5. The threading dislocation density obtained after annealing at 1000 °C or at high implantation doses is always larger than 10^9 cm^{-2}, which is unacceptably high for any device application. A minimum threading dislocation density of about 10^7 cm^{-2} is observed for a He implantation dose of 2.0×10^{16} cm^{-2} and an annealing temperature of 850 °C.

In contrast to annealed samples, the as-implanted sample implanted with 2×10^{16} cm^{-2} does not reveal any structural defects, neither dislocations nor He bubbles.

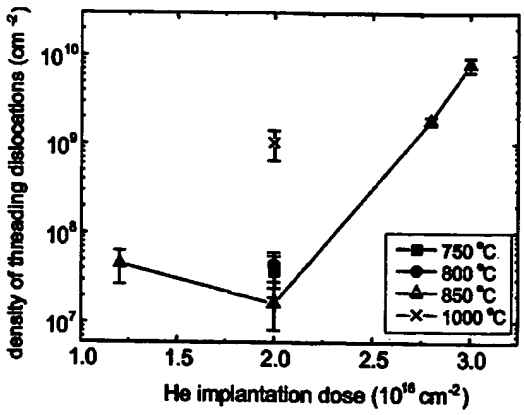

FIG. 5. Threading dislocation density plotted vs the He implantation dose for the different annealing temperatures indicated.

IV. DISCUSSION

Two aspects of the effect of He implantation and annealing on the relaxation of SiGe/Si heterostructures will be discussed below. First, we will address the formation of He bubbles within the Si substrate. Second, we will focus on the relaxation mechanism of the SiGe layers in the presence of the He bubbles acting as internal dislocation sources.

The formation of He bubbles in Si is a complex phenomenon, since several processes depending on annealing time, temperature, and implantation parameters are involved, like nucleation, decomposition, and He desorption. According to Fichtner *et al.*[18] three regimes of different nucleation and growth phenomena can be distinguished: At low He concentration ($<1\times10^{16}$ cm^{-2}) He_nV_m clusters of n He atoms and m vacancies (V) are formed, which dissociate at low annealing temperature (<400 °C).[19] At high He concentration ($>2\times10^{16}$ cm^{-2}), bubbles are already formed during implantation and follow a coarsening process during annealing.[20] Finally, in the intermediate He concentration regime the microstructure is strongly dependent on the annealing temperature, the as-implanted sample being free of any extended defects and He bubbles. Annealing at low temperatures (≈300 °C) results in platelike He precipitates, which are heavily overpressurized as indicated by the surrounding strain fields.[21] At this stage the formation of dislocation loops surrounding the platelets was observed. Annealing at higher temperatures (600 °C) results in a decomposition of the platelets into spherical bubbles, which are still surrounded by strain fields owing to the overpressurized state of the bubbles. Only upon high temperature anneals (>700 °C) is the pressure within the bubbles released by desorption of He.[20]

Clearly, at low doses ($\leq2\times10^{16}$ cm^{-2}) our case is characterized by "intermediate He concentrations," since no bubble-like structures can be detected in the as-implanted sample. The independence of the bubble diameter of implantation dose (Fig. 2) indicates coarsening of the bubbles by Ostwald ripening during annealing, according to theoretical considerations[22] and experimental studies on He bubbles in metals.[23] Obviously, the bubble structures (Fig. 1) formed during annealing can be considered as a late state of their evolution, since no strain fields can be observed. Therefore, part of the He seems to be released by annealing. However, according to literature, in the early stages overpressurized bubbles or platelets are formed, which act as dislocation sources. Indeed, we find some dislocations within the layer and, more importantly, a considerably higher density of misfit dislocations within the SiGe/Si interface compared to unimplanted and annealed only samples.

The role of He bubbles as internal dislocation sources is the key to producing relaxed SiGe layers on Si substrates with only few threading dislocations. Conventional relaxation of heterostructures through annealing involves the heterogeneous generation of dislocations at internal dislocation sources such as grown-in dislocations or at the surface of the epilayer, which glide into the interface and thereby relax the layer.[24] If this procedure is imposed on our samples, the maximum degree of relaxation achievable is about 35% only

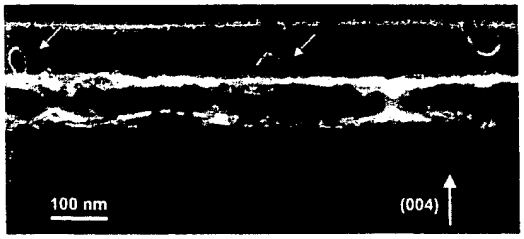

FIG. 6. Weak beam dark field electron micrograph in cross section of a sample implanted with 2×10^{16} cm^{-2} and annealed at 1000 °C. The bubble layer and the interface show blurred white contrast according to the strain fields of dislocations. Clearly, two dislocation loops can be seen to be generated within the sample, whereas a half loop is attached to the surface.

(see Fig. 3 and Table 1). Introducing He bubbles into the Si substrate improves the degree of relaxation by a factor of 2. Evidence for dislocation loop generation from internal sources is given in Fig. 6. The weak beam dark field image shows two dislocation loops extending from the SiGe/Si interface into the epilayer, whereas one dislocation loop is evidently formed at the surface. Thus, two relaxation mechanisms are active in this particular sample, implanted with 2×10^{16} cm^{-2} and annealed at a very high temperature of 1000 °C.

Recently, the strain relaxation by H and He implantation of SiGe/Si heterostructures was described in a theoretical model,[25] which suggests that the strain relaxation was initiated by dislocation loops punched out by the He filled overpressurized bubbles within the Si substrate. These loops glide to the interface. When a loop comes into contact with the SiGe layer it experiences an asymmetric force. As a consequence, one side of the loop is pinned at the interface where it forms a strain relieving misfit segment. The other side is driven by the mismatch stress to the surface where an atomic step is generated. The accompanied threading dislocations from different loops annihilate efficiently by a combined climb–glide mechanism. Obviously the density of dislocation sources, i.e., He bubbles, has to be sufficiently high to allow generation of a large number of misfit dislocations to relax the SiGe layer. In addition, the distance between threading dislocations has to be smaller than the annihilation radius of two dislocations with opposite Burgers vectors. Trinkaus *et al.*[25] quantified two conditions necessary for effective relaxation and complete annihilation of threading dislocations: $\delta \leq 2.5d$ and $\delta \leq h$, where δ is the distance between precipitates, d the bubble diameter, and h the thickness of the epilayer.

These conditions appear to be well fulfilled for all our samples: Taking the implantation series (see Table I) as an example, δ varies between 13 and 49 nm, which is within the margin of errors smaller than or equal to 2.5 $d=(38\pm12)$ nm. Thus, even samples with high He implantation doses and/or high annealing temperatures seem to fulfill the conditions required by the model. However, in these cases the annihilation of the threading dislocations does not work efficiently. This may indicate that the conventional relaxation mechanism still operates (see Fig. 6), introducing threading dislocations, which cannot effectively annihilate. In addition, these samples contain a considerable density of bubbles within the interface. These react with the dislocations[26] and therefore impede motion of the threading dislocations necessary for annihilation.

It is important to point out that the initial overpressure within the bubbles is not known to date, which prevents quantitative evaluation of their strength as dislocation sources. Since the bubbles observed in the present study do not exhibit strain fields, dislocation formation must occur in an earlier stage of the bubble evolution, where the stress imposed by an overpressurized bubble is larger than the critical shear stress for dislocation formation. Indeed, dislocation loops have been reported to form already at temperatures as low as 350 °C, where the bubbles still have their platelet shape.[18] Therefore, assuming the dislocation generation in the "platelet stage," the density of dislocation sources can be considerably lower as deduced from the density of spherical bubbles, since the mean distance between platelets is larger than the spacing between bubbles observed at a later stage. In consequence, an effective dislocation source density has to be considered in the model[25] to quantitatively describe the relaxation mechanism. Qualitatively, our experimental observations of the bubble structure and of the types of dislocations are in agreement with the model.

V. CONCLUSION

In conclusion, a high degree of relaxation of thin SiGe layers grown on Si (100) substrates can be achieved by He implantation and subsequent annealing at relatively moderate annealing temperatures. The dislocation generation necessary for relaxation of the $Si_{0.7}Ge_{0.3}$ layer is induced by the presence of overpressurized He filled precipitates. At a dose of 2.0×10^{16} cm^{-2} and an annealing temperature of 850 °C a threading dislocation density as low as 10^7 cm^{-2} is obtained. Therefore, He implantation and subsequent annealing are promising techniques to achieve good quality strain-relaxed SiGe grown on Si (100), even for layers with Ge concentrations of as high as 30%. Such wafers are highly attractive as virtual substrates for Si/SiGe based high speed/high performance devices in Si technology. The advantages compared to thick strain relaxed buffer layers are quite obvious: The small thickness of the SiGe film poses no problems in technology and, especially important, it minimizes the problem of low thermal conductivity of SiGe alloys.

ACKNOWLEDGMENTS

The authors would like to thank M. Gebauer for performing the ion implantations and H. Schwalbach and P. Pickartz for the assistance during RBS measurements. Part of this work was supported by the European Community under the IST Program, Project No. SIGMUND.

[1] U. König and M. Glück, J. Vac. Sci. Technol. B **16**, 2609 (1998).
[2] F. Schäffler, Semicond. Sci. Technol. **12**, 1515 (1997).
[3] H.-J. Herzog, T. Hackbarth, G. Höck, M. Zeuner, and U. Koenig, Thin Solid Films **36**, 380 (2000).
[4] G. Bai, M.-A. Nicolet, C. H. Chern, and K. L. Wang, J. Appl. Phys. **75**, 4475 (1994).
[5] F. K. LeGoues, K. Eberl, and S. S. Iyer, Appl. Phys. Lett. **60**, 2862 (1992).

[6] E. A. Fitzgerald, Y.-H. Xie, D. Monroe, P. J. Silverman, J. M. Kuo, A. R. Kortan, F. A. Thiel, and B. E. Weir, J. Vac. Sci. Technol. B **10**, 1807 (1992).
[7] M. Honisch, H.-J. Herzog, and F. Schäffler, J. Cryst. Growth **157**, 126 (1995).
[8] A. R. Powell, S. S. Iyer, and F. K. LeGoues, Appl. Phys. Lett. **64**, 1856 (1994).
[9] B. Holländer, S. Mantl, W. Michelsen, St. Mesters, A. Hartmann, L. Vescan, and D. Gerthsen, Nucl. Instrum. Methods Phys. Res. B **84**, 218 (1994).
[10] K. K. Linder, F. C. Zhang, J.-S. Rieh, P. Bhattacharya, and D. Houghton, Appl. Phys. Lett. **70**, 3224 (1997).
[11] K. Lyutovich, F. Ernst, E. Kasper, M. Bauer, and M. Oehme, Solid State Phenom. **69–70**, 179 (1999).
[12] T. Hackbarth, H.-J. Herzog, M. Zeuner, G. Höck, E. A. Fitzgerald, M. Bulsera, C. Rosenblad, and H. von Känel, Thin Solid Films **369**, 148 (2000).
[13] S. Mantl, B. Holländer, R. Liedtke, St. Mesters, H.-J. Herzog, H. Kibbel, and T. Hackbarth, Nucl. Instrum. Methods Phys. Res. B **147**, 29 (1999).
[14] B. Holländer, St. Lenk, S. Mantl, H. Trinkaus, D. Kirch, M. Luysberg, T. Hackbarth, H.-J. Herzog, and P. F. P. Fichtner, Nucl. Instrum. Methods Phys. Res. B **175–177**, 357 (2001).
[15] M. Luysberg, D. Kirch, H. Trinkaus, B. Holländer, St. Lenk, S. Mantl, H.-J. Herzog, T. Hackbarth, and P. F. P. Fichtner, Inst. Phys. Conf. Ser. **169**, 181 (2001).
[16] S. H. Christiansen, P. M. Mooney, J. O. Chu, and A. Gril, Mater. Res. Soc. Symp. Proc. **686**, A1.6.1 (2002).
[17] Although we cannot verify with our experimental methods that the spherical cavities contain He (and even worse in which aggregate state), we nonetheless use the term "He bubble" which has been established in literature to describe implantation induced He precipitation. According to Ref. 19 we can safely assume that for annealing temperatures $<1000\,^{\circ}C$ the cavities are still partly filled with He.
[18] P. F. P. Fichtner *et al.*, Nucl. Instrum. Methods Phys. Res. B **136–138**, 460 (1998).
[19] A. Van Veen, H. Schut, R. A. Hakvoort, A. Fedorov, and K. T. Westerduin, Mater. Res. Soc. Symp. Proc. **373**, 499 (1995).
[20] C. C. Griffeon, J. H. Evans, P. C. de Jong, and A. van Veen, Nucl. Instrum. Methods Phys. Res. B **27**, 417 (1987).
[21] P. F. P. Fichtner, J. R. Kaschny, R. A. Yankov, A. Mücklich, and U. Kreißig, Appl. Phys. Lett. **61**, 2656 (1996).
[22] H. Trinkaus, Radiat. Eff. **78**, 189 (1983).
[23] H. Schroeder, P. F. P. Fichtner, and H. Trinkaus, in *Fundamental Aspects of Inert Gases in Solids*, edited by S. E. Donelly and J. H. Evans (Plenum New York, 1991).
[24] E. A. Fitzgerald, Mater. Sci. Rep. **7**, 87 (1991).
[25] H. Trinkaus, B. Holländer, St. Rongen, S. Mantl, H.-J. Herzog, J. Kuchenbecker, and T. Hackbarth, Appl. Phys. Lett. **76**, 3552 (2000).
[26] D. M. Follstädt, S. M. Myers, and S. L. Lee, Appl. Phys. Lett. **69**, 2059 (1996).